https://doi.org/10.5194/egusphere-2026-4781
Preprint. Discussion started: 18 August 2026

A comparison of metrics for CO_2 uptake efficiency of regional ocean alkalinity enhancement in an Earth system model

Vanessa Teske[1], Tronje Kemena[1], and Andreas Oschlies[1]
[1]GEOMAR Helmholtz-Zentrum for Ocean Research Kiel, Kiel, Germany
Correspondence: Vanessa Teske (vteske@geomar.de)

Abstract. Ocean Alkalinity Enhancement (OAE) is a method proposed for ocean-based Carbon-Dioxide Removal and describes the sequestration of CO_2 from the atmosphere through a deliberate increase in alkalinity in the ocean. In this study, we compare multiple approaches for the calculation of the CO_2 uptake efficiency for regional OAE using an Earth system model. We find that for regional alkalinity deployment at the European Atlantic coast the change in the global ocean inventories for dissolved inorganic carbon and alkalinity is not a feasible approach. The OAE-induced removal of CO_2 from the atmosphere leads to phase shifts in the large-scale climate pattern El Niño, but it does not influence its frequency or intensity. This alters the timing of interannual variations in global carbon fluxes, which obscures the detection of the immediate signal of alkalinity addition on ocean carbon uptake on annual to decadal timescales. Approaches that track the regional distribution of the added alkalinity or the OAE-induced regional strengthening of the air-sea CO_2 flux provide more robust estimates of CO_2 uptake efficiency, when the following criteria are taken into account: (i) ocean conditions in and close to the deployment region (e.g., circulation, upwelling and subduction) (ii) the natural variability of surface alkalinity and air-sea CO_2 flux, and (iii) the possible impacts on global climate modes such as El Niño.

1 Introduction

The cumulative ocean carbon sink is estimated to be 170±35 GtC between 1850 and 2020 (Friedlingstein et al., 2022). However, the fraction of CO_2 emissions taken up by the ocean in the future is difficult to predict, possibly increasing to 290±30 GtC under the emission scenario SSP1-2.6 and 520±40 GtC under SSP5-8.5 by 2100 (Liddicoat et al., 2021; Canadell et al., 2021). With ongoing climate warming, the task of reducing global emissions is becoming increasingly pressing. To halt global warming, net zero CO_2 emissions needs to be achieved, in turn requiring strong emission reduction complemented by CO_2 removal from the atmosphere to balance the remaining hard-to-abate emissions. Traditionally, most CO_2 removal (CDR) methods considered have been terrestrial methods, but it is increasingly becoming clear that their potential and upscaling speed will make it difficult to reach CDR amounts sufficient to reach net-zero emissions by mid century, as deemed necessary to limit warming to less than 2°C (UNFCCC, 2015). With the ocean being the largest carbon reservoir exchanging carbon with the atmosphere on societally relevant timescales, it appears reasonable to carefully consider marine CDR approaches as well (Oschlies et al., 2025).

https://doi.org/10.5194/egusphere-2026-4781
Preprint. Discussion started: 18 August 2026

Ocean Alkalinity Enhancement (OAE) is a method for marine CDR (mCDR) with promising potential to make a significant contribution to the total demand of CDR. It is described as the sequestration of CO_2 from the atmosphere through a deliberate increase in alkalinity in the surface ocean (Renforth and Henderson, 2017).

To evaluate the effectiveness of OAE as an mCDR method, its efficiency is defined as the amount of CO_2 sequestered per unit of added alkalinity (Schwinger et al., 2024). It is commonly calculated as the ratio of volume-integrated increases in ocean dissolved inorganic carbon (DIC) to the cumulative added alkalinity. The metric was introduced by Renforth and Henderson (2017) and links the efficiency of OAE to the chemical buffer capacity of the ocean. The explicit formulation of this ratio appears under different synonyms in the literature; it is called long-term efficiency (Nagwekar et al., 2024), chemical efficiency (Schwinger et al., 2024), carbon-uptake efficiency or carbon-uptake potential (Burt et al., 2021; He and Tyka, 2023).

An alternative approach to calculate the OAE efficiency employs the cumulative air-sea CO_2 flux (Nagwekar et al., 2024). When considering idealized global-scale application of OAE, as commonly assumed by global modelling studies so far, OAE-induced changes in global ocean DIC inventory should very closely match OAE-induced changes in cumulative air-sea CO_2 fluxes - with small differences being possibly caused by net transformations between DIC and organic carbon in the water column. For either way of measuring efficiency, Schwinger et al. (2024) differentiate between Earth system efficiency – simulations including carbon-cycle climate feedbacks – and capture efficiency, which is a result of simulations without carbon-cycle climate feedbacks. In both cases, the globally integrated cumulative air-sea CO_2 flux, or the change in DIC content, is set in relation to the cumulative added alkalinity.

Although these approaches are straightforward to implement in numerical models, the metrics to calculate efficiency listed above without any other constraints have some caveats. The use of increases in global-ocean DIC and added alkalinity (ALK_{add}) has been shown to work well for large-amplitude hypothetical global OAE applications (Schwinger et al., 2024). However, in a reasonably more realistic regional OAE application (e.g., river sources, small coastal areas), the OAE signal in the global DIC and alkalinity changes might be very small compared to background variability, as both DIC and alkalinity vary due to internal and anthropogenically-driven climate and ocean variability. Global-ocean DIC content varies as a result of anthropogenic CO_2 uptake and internal climate modes, such as El Niño. Alkalinity varies through changes in biological and chemical processes including calcification and carbonate dissolution, denitrification, and nitrogen fixation (Paulmier et al., 2009). This noise caused by internal model variability is particularly relevant for Earth system models with fully coupled carbon cycle and interactive atmospheric CO_2 that responds to changes in carbon fluxes.

In this study, we apply OAE in a regional setting within a confined European coastal region to a fully coupled atmosphere–ocean general circulation model under a high CO_2 emission scenario with an interactive carbon cycle. The signal of CO_2 removal induced by small-scale regional alkalinity addition, however, is likely to be masked by both strong background emissions and internal climate variability, resulting in a low signal-to-noise ratio. In such a setting, robust efficiency metrics are required to reliably detect and quantify carbon removal efficiency under real-world conditions.

We compare multiple metrics for the calculation of the CO_2 uptake efficiency of regional OAE simulated with an Earth system model, and discuss what speaks for and against certain methods in establishing guidelines for future work and the comparability between different studies and observations.

https://doi.org/10.5194/egusphere-2026-4781
Preprint. Discussion started: 18 August 2026

2 Methods

We run experiments with the FOCI Earth system model (Matthes et al., 2020). The main components of the model are the ocean model Nucleus for European Modelling of the Ocean (NEMO3.6) (Madec and the NEMO team, 2016), the European Center Hamburg general circulation model (ECHAM6) for the atmosphere (Stevens et al., 2013), including a land model JSBACH for the carbon cycle on land and TRACY-MOPS for the biogeochemistry of the ocean (Chien et al., 2022; Kriest and Oschlies, 2015). The ocean grid has a global resolution of 1/2° on a tripolar grid with a 1/10° resolution nest in the North Atlantic (Fig. 1). The grid has 46 vertical levels ranging from the thickness of 6 m near the surface to the thickness of 250 m in the deep ocean. The atmosphere has run with a T63 spectral resolution, corresponding to a Gaussian grid of approximately 1.8° x 1.8°, in a low-top atmosphere with 95 vertical layers and with interactive atmospheric CO_2 represented as a prognostic three-dimensional tracer. The atmosphere-land component ECHAM6-JSBACH and the ocean–biogeochemistry component NEMO-MOPS are fully coupled via OASIS3-MCT, enabling e.g. the exchange of CO_2 between the ocean, land, and atmosphere, which allows for carbon-cycle feedbacks.

The simulations are performed with the Shared Socioeconomic Pathway SSP3-7.0 emission scenario, which includes projected socio-economic developments as well as atmospheric greenhouse gas concentrations (Meinshausen et al., 2020). The model uses idealized, completely dissolved alkalinity to simulate OAE experiments. To investigate the behaviour of alkalinity distribution and changes in the ocean carbon uptake, simulations are performed where the alkalinity was added in eight separate coastal regions (Fig. 1a). The coastal regions are separated by country: United Kingdom (UK, blue), Spain and Portugal (SP & PT, orange), Norway and Sweden (NOR & SW, green), the Netherlands and Belgium (NE & BE, red), Ireland (IRE, violet), Iceland (ICE, brown), Germany and Denmark (GER & DK, pink), and France (FR, grey). The alkalinity addition ALK_{ADD} follows a linear ramp up for the first 10 years from year 2025 to 2034 until the total ocean alkalinity addition over all coastal sections adds up to the equivalent of 1 Gt $Ca(OH)_2$/year (27 Tmol/year alkalinity), distributed uniformly over the entire coastal deployment area, an approx. 50 km wide stripe along the coast. From 2035 to 2049, a continuous addition of alkalinity at a steady rate is simulated (Fig. 1b). Based on the latest assessments, current implemented climate policies lead to emissions analogue to an emission scenario somewhere between SSP2-3.4 and SSP2-4.5 (Burgess et al., 2023; United Nations Environment Programme, 2025), where European emissions reach 8 Gt CO_2/year to 13.3 Gt CO_2/year in 2050 (Riahi et al., 2017). In an ideal case, approx. 1 Gt $Ca(OH)_2$/year would be needed to remove approx. 0.8 Gt CO_2/year from the atmosphere (Foteinis et al., 2022). While this is only about 10% of the projected European emissions for SSP2-3.4 in 2050, 1 Gt $Ca(OH)_2$ is a bit less than five times the amount of $Ca(OH)_2$ produced by the European cement industry in 2021 (approx. 220 Mt $Ca(OC)_2$; CEMBUREAU, 2023). While the total amount of 27 Tmol alkalinity is too large to be realistically achievable, the alkalinity additions to single coastal segments are comparatively more feasible (Fig. 1b). In addition to the OAE simulations, one simulation without any alkalinity addition was performed as a baseline (BASE).

https://doi.org/10.5194/egusphere-2026-4781
Preprint. Discussion started: 18 August 2026

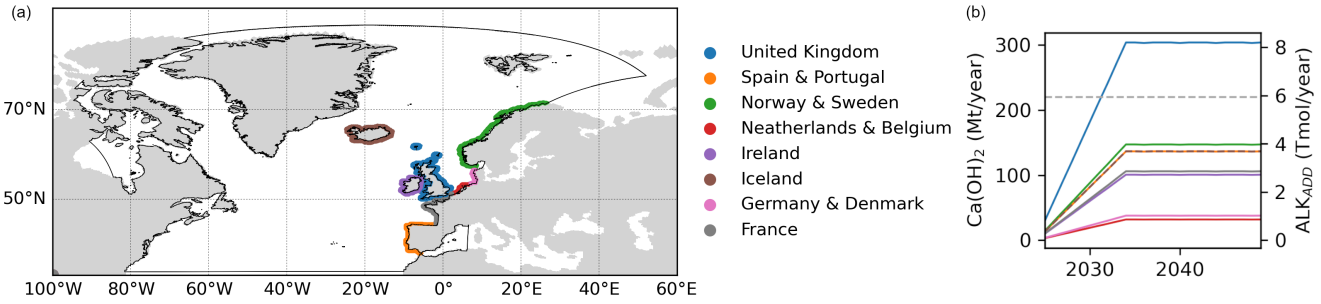

Figure 1. (a) Nest domain in the North Atlantic outlined in black. Coloured areas show deployment regions for alkalinity in the different simulations. (b) Yearly rate of alkalinity addition and the equivalent of $Ca(OH)_2$. The approximate amount of $Ca(OH)_2$ produced by the European cement industry in 2021 is shown as a dashed gray line (CEMBUREAU, 2023).

2.1 CO_2 uptake efficiency based on DIC and alkalinity budgets

For the first method, we calculate changes in the inventories of DIC and alkalinity of the ocean between the OAE simulations and BASE:

$$EFF(t) = \Delta DIC(t)/\Delta ALK(t) \tag{1}$$

(i) Global budgets: The total changes in global-ocean DIC and alkalinity due to OAE are diagnosed as differences between OAE simulations and BASE.

(ii) Coastal budget: Only the water column below the grid nodes where alkalinity is applied, is used to calculate changes in ocean alkalinity and DIC between OAE simulations and BASE.

(iii) Threshold-based budgets: Different thresholds (10, 20, 50, 100 μmol/kg) are applied to the difference in surface alkalinity between the OAE experiments and BASE at each of the surface nodes. This allows to restrain the calculation to the region of spreading of the alkalised water masses. To ensure that only DIC anomalies are counted that are related to OAE, we apply a spatial connectivity criterion: The initial "seed" region is defined by the alkalinity deployment zones along the European coast. For each year beginning with the start of OAE deployment, we identify connected grid cells (using 4-neighbour grid adjacency) where the surface alkalinity anomaly (ΔALK) exceeds the respective threshold and is connected to the OAE deployment region. For time steps, where the threshold is not exceeded, the relevant grid cells are again removed from the calculation. The DIC anomaly (ΔDIC) is then integrated only over the region of alkalinity anomalies connected to the OAE deployment region. This approach aims to follow the physical spread of the added alkalinity as a result of horizontal transport.

https://doi.org/10.5194/egusphere-2026-4781
Preprint. Discussion started: 18 August 2026

2.2 CO_2 Uptake Efficiency based on cumulative Air–Sea Flux Anomalies

As a second approach we calculate the CO_2 uptake efficiency as the ratio of time-integrated anomalous air–sea CO_2 flux to the cumulative alkalinity added (Eq. 2). The flux anomaly is calculated at each grid cell and time step as the difference between the OAE simulation and the BASE run, representing the additional net CO_2 uptake caused by OAE. Both the anomalous CO_2 flux and the added alkalinity are integrated over time to yield annual cumulative efficiency values.

$$EFF(t_1) = \sum_{0}^{t_1} \Delta F_{CO_2}(t)\, dt / \sum_{0}^{t_1} ALK_{ADD}(t)\, dt \tag{2}$$

We restrict the analysis to statistically significant anomalous CO_2 fluxes, applying two different criteria to identify the fraction of the air–sea CO_2 flux attributable to OAE, while removing natural variability and noise as far as possible. To account for temporal consistency and spatial coherence, we implement a time-of-emergence (TOE) approach to detect when and where the OAE signal rises above natural variability, combined with a connectivity filter to restrict the analysis to physically connected impact regions. At each model grid cell, we perform a moving-window statistical test on the CO_2 flux anomaly. Specifically, we apply a two-sample, one-tailed t-test over a 5-year sliding window to determine whether the annual mean CO_2 flux under OAE is significantly lower than in the control simulation BASE. A significance level of $\alpha = 0.01$ is used. Each time step in which a statistically significant negative anomaly occurs is recorded as the point of signal emergence for that grid cell. This approach is conceptually analogous to determining the TOE of a forced climate signal from internal variability (Turk et al., 2019). Additionally, the spatial connectivity criterion described above is applied to the flux anomaly. Any newly significant grid cell adjacent to the existing connected region is added, while grid cells that show no significant difference any more are remove. This method was also applied to ΔALK, but no areas could be identified where the t-test yielded statistically significant results at either the 0.01 or 0.05 significance level. Therefore, the threshold criterion in section 2.1.(iii) was used instead.

2.3 Combined plume tracking criteria

To be able to directly compare the uptake efficiency calculated over the same volume, we combine the threshold criterium for surface alkalinity changes and the significance criterium for the air-sea flux changes. The CO_2 uptake efficiency is then calculated based on (i) the ratio of ΔDIC to ΔALK (Eq. 1), and (ii) the ratio of the cumulative air-sea flux changes to ALK_{ADD} (Eq. 2).

3 Results

3.1 Budget changes of alkalinity and dissolved inorganic carbon

The reference simulation BASE shows changes in the total amount of alkalinity and DIC in the ocean over the course of the 25 simulated years. While the alkalinity content of the ocean decreases slightly by approx. 0.07 Pmol between 2025 and 2049, the amount of DIC shows an increase by approx. 6.52 Pmol in the high-emission SSP3-7.0 scenario, with overlaid seasonal

https://doi.org/10.5194/egusphere-2026-4781
Preprint. Discussion started: 18 August 2026

variations. Most of the additional carbon is taken up by the Atlantic Ocean, visible as increased DIC content between the equator and approx. 45°N (Fig. S1). In contrast, some regions in the subtropical Pacific and Indian Ocean experience lower DIC caused by outgassing in the respective regions. The change in alkalinity is more evenly distributed with some increase in alkalinity in the eastern and northern Pacific, while the Atlantic Ocean is dominated by alkalinity loss. These changes are caused by the increasing CO_2 concentration in the atmosphere. The higher concentration increases the partial pressure of CO_2 (pCO_2) towards the ocean surface and strengthens the CO_2 flux into the ocean.

a) *Global ocean*

The easiest way to make sure that all OAE-induced DIC changes are accounted for in the efficiency calculation, is to include the global ocean when calculating ΔALK and ΔDIC. In an idealized scenario without feedback effects between the different climate components, the alkalinity in the ocean accumulates over time in the OAE simulations and increases by the same amount as ALK_{ADD}. Similarly, ΔDIC increases over time. However, the model simulations show that neither is ΔALK identical to ALK_{ADD} (Fig. 2a), nor does ΔDIC follow proportionally (Fig. 2b), except for the simulation with OAE application along the whole EU coast (EU; inset in Fig. 2a and b).

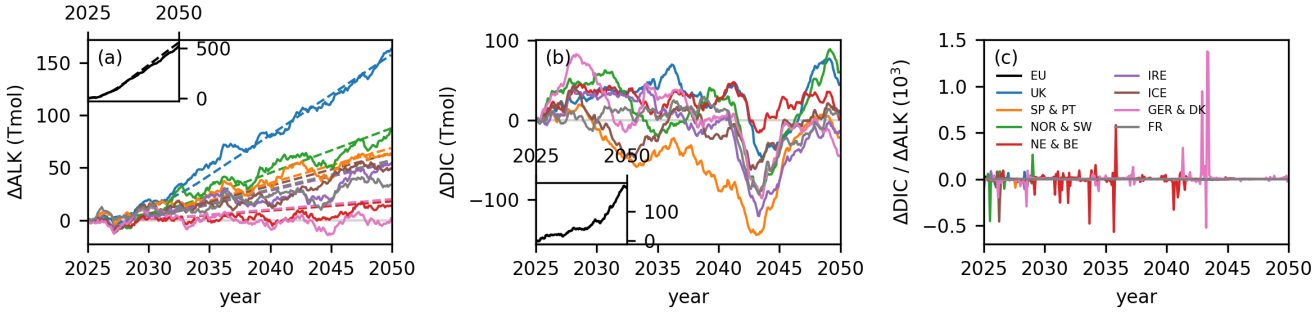

Figure 2. Global ocean budgets. (a) Change in global alkalinity content relative to the baseline simulation, dashed lines show the accumulated alkalinity additions ALK_{ADD} for each simulation ($\sum_0^{t_1} ALK_{ADD}(t)\,dt$). (b) Change in global DIC content, (c) CO_2 uptake efficiency ($\Delta DIC/\Delta ALK$) for the global ocean. Insets in (a) and (b) show ΔALK and ΔDIC for the simulation with alkalinity addition along the whole European coast (EU).

In the simulations with regional OAE forcing ΔDIC becomes negative over large time spans, indicating reduced carbon uptake by the ocean compared to the reference simulation BASE despite the addition of alkalinity (Fig. 2a). The largest differences in ocean DIC can be found in the tropical Pacific Ocean (not shown). Differences in CO_2 outgassing and CO_2 uptake brought about by phase shifts in the El Niño/La Niña events accumulate in the DIC reservoir of the ocean (Fig. 3a); during El Niño events, higher sea surface temperatures lead to enhanced outgassing, while colder sea surface temperatures during La Niña lead to a stronger CO_2 uptake (Sun et al., 2025). The effect is confirmed by a strong correlation between the cumulative Niño3.4 index (Fig. 3b), calculated from sea surface temperature anomalies in the equatorial Pacific Ocean, and the global ΔDIC (Pearson coefficients: 0.63-0.86, r<0.01). The change in DIC due to OAE is masked by the much larger effect of the shift in El Niño/La Niña events on year-to-year changes in the oceanic DIC inventory in nearly all OAE simulations, rendering

https://doi.org/10.5194/egusphere-2026-4781
Preprint. Discussion started: 18 August 2026

ΔDIC of the global ocean relatively insensitive for the calculation of CO_2 uptake efficiency of regional OAE applications on annual to multi-decadal timescales. The only exception is the EU simulation, where the additional OAE-induced carbon uptake is large compared to the cumulative effect of El Niño on the carbon cycle, resulting in a net increase in global ocean DIC.

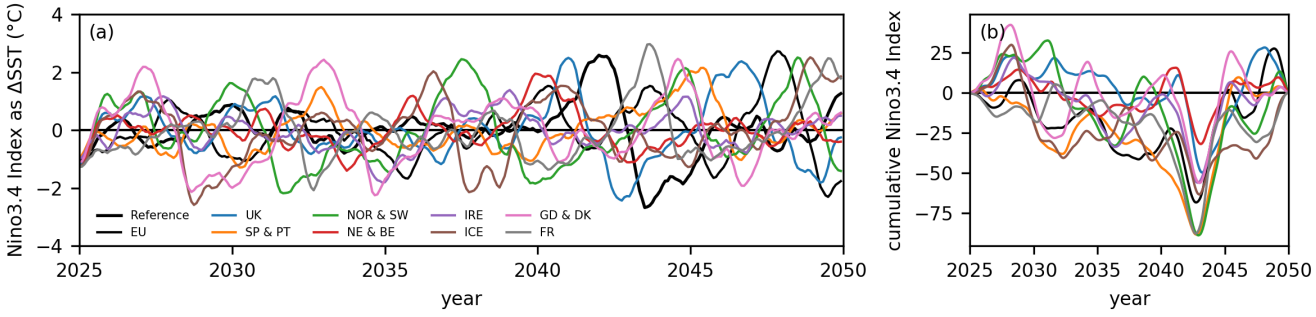

Figure 3. a) Niño3.4 index from sea surface temperature anomalies in the index region Niño3.4. b) Cumulative change of the Niño3.4 index difference between the OAE experiments and the reference run.

The differences between ΔALK and ALK_{ADD} shown in Fig. 2a are caused by OAE-induced changes in biogeochemical processes, in particular the formation and consumption of nitrate and phosphate via microbial activity, including denitrification and nitrogen fixation with subsequent nitrification (Paulmier et al., 2009). These changes occur in response to OAE-induced changes in the state of the climate system. They can lead to differences in globally integrated nitrate content that strongly correlate negatively with the difference between ΔALK and ALK_{ADD} (Pearson coefficients: -0.51 – -0.97, r<0.01) because an increase of nitrate is accompanied by a decrease of alkalinity (Chien et al., 2022). Changes in phosphate content can, in the current model version, arise only from changes in the partitioning of the conserved total phosphorus inventory among inorganic phosphate and particulate or dissolved organic phosphorus. Both denitrification and nitrogen fixation occur generally far away from the regional OAE deployment in our simulations, but can affect the global ocean nitrate inventory. In the OAE experiments with small alkalinity additions like the runs with alkalinity addition at the coasts of the Netherlands and Belgium (NE & BE) or Germany and Denmark (GER & DK), the effect of the changing nutrient inventories on alkalinity are of a similar scale as the addition of ALK_{ADD} itself. Given out-of-phase interannual variations in OAE and BASE runs, this occasionally leads to ΔALK values close to zero, resulting in spikes in uptake efficiencies when diagnosed from the global ΔDIC/ΔALK ratio (Fig. 2c).

b) *Coastal ocean*

One option to reduce the effects of OAE-induced remote impacts on the fixed nitrogen and alkalinity budgets on the diagnosed CO_2 uptake efficiency of regional OAE is to constrain the region for which the efficiency is diagnosed to the actual alkalinity deployment region (Fig. 4a, compare to map in Fig. 1). Of the accumulated alkalinity addition, less than 2.5 % stay within the local water column over the 25 years of the experiment. The lion's share is exported. In contrast to the global reservoir, the

https://doi.org/10.5194/egusphere-2026-4781
Preprint. Discussion started: 18 August 2026

change in ocean DIC in these areas is positive and can be directly related to the alkalinity increase (Fig. 4b). The resulting efficiencies range from 0.16±0.17 in the simulation with additions in Norway and Sweden (NOR & SW) to 0.53±0.03 for EU.

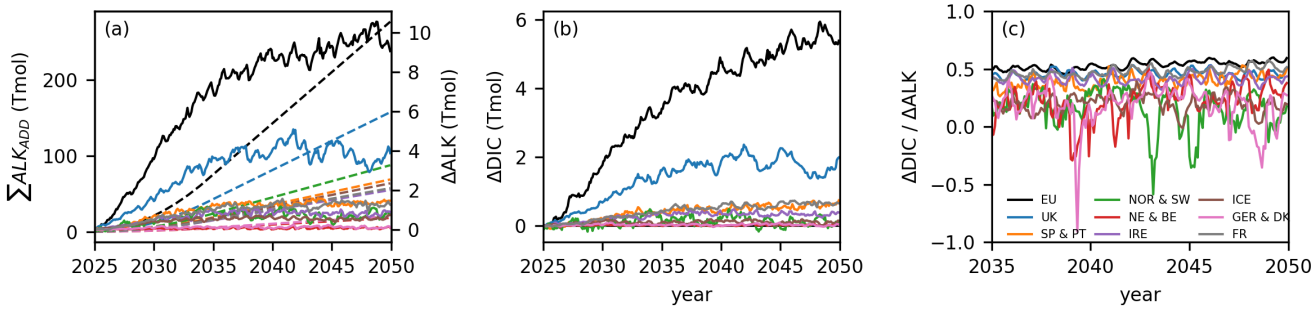

Figure 4. Coastal oceans. (a) Dashed lines show the accumulated alkalinity additions (right axis). Solid lines show the change in alkalinity content in the water column in the OAE deployment region along the coasts (left axis). (b) Change in DIC content in the water column in the same region. (c) CO_2 uptake efficiency between 2035 and 2050. Due to values of ΔALK close to zero between 2025 and 2035, the efficiency far exceeds reasonable values and has been excluded from the analysis.

c) *Spreading of alkalised water masses*

The alkalised water masses spread along the European coast (Fig. S2). While alkalinity additions in the North Sea are mostly transported North towards the Arctic Ocean and stay close to the coast, alkalised water masses originating at the coasts of Portugal and Spain are also circulated into the Mediterranean Sea. When diagnosing the efficiency over the region of the expanding plume of alkalised water, the choice of threshold for the change in surface alkalinity concentration in the plume definition strongly influences the resulting diagnosed efficiency (Table 1). For a low threshold (10 μmol/kg), the average efficiency ranges from 0.36±0.12 for Iceland (ICE) to 0.74±0.17 for the addition along the coasts of the Netherlands and Belgium (NE & BE). For higher thresholds, the areas included in the calculation reduce, but efficiencies can go up. For the four thresholds explored in this analysis, the simulations for EU and ICE show the highest efficiency for a threshold of 20 μmol/kg, while FR and NOR & SW show highest efficiencies for an even higher threshold of 50 μmol/kg. However, when the threshold is too high, the plume area is underestimated because the change in alkalinity concentration rarely exceeds the threshold.

The probability density functions (calculated with the python package diffKDE by Pelz et al., 2023; Pelz and Slawig, 2024) of the interannual variability of the surface alkalinity concentration in BASE shows a probability up to 35% for the surface alkalinity to be 10 μmol/kg larger than the 25 year mean in the North Sea and along the Norwegian coast (Fig. 5a). When the interannual variability is of similar scale or larger than the detection threshold for the plume of alkalised water mass, noise is introduced to the efficiency calculation. If the concentration threshold is chosen too low, areas of high background variability are included in the region labelled as alkalinity plume; the calculated efficiency then includes noise and represents an artificial efficiency of the variability instead of the effect of OAE. With a threshold that is higher than the internal variability,

https://doi.org/10.5194/egusphere-2026-4781
Preprint. Discussion started: 18 August 2026

Table 1. Mean CO_2 uptake efficiencies and temporal standard deviation calculated over the expanding plume of alkalised water based on four different thresholds to constrain the area applied to the surface alkalinity concentration.

	$\sum \Delta F_{CO_2} / \sum ALK_{ADD}$	ΔDIC/ΔALK				
		coast	10 μmol/kg	20 μmol/kg	50 μmol/kg	100 μmol/kg
EU	0.591	0.532	0.641±0.088	0.670±0.104	0.656±0.068	0.640±0.069
UK	0.598	0.458	0.651±0.074	0.645±0.085	0.639±0.078	0.592±0.059
SP&PT	0.509	0.398	0.555±0.180	0.553±0.156	0.512±0.150	0.432±0.065
NOR&SW	0.582	0.159	0.468±0.213	0.390±0.250	0.414±0.177	0.218±0.081
NE&BE	0.595	0.217	0.739±0.165	0.664±0.090	0.520±0.072	0.409±0.080
IRE	0.597	0.411	0.651±0.125	0.616±0.142	0.602±0.080	0.542±0.035
ICE	0.310	0.202	0.360±0.117	0.387±0.177	0.215±0.046	0.202±0.036
GER&DK	0.504	0.185	0.629±0.276	0.527±0.177	0.386±0.155	0.295±0.142
FR	0.608	0.474	0.587±0.128	0.573±0.134	0.637±0.106	0.574±0.099

the detection becomes more robust, noise is reduced, and the characteristics of the coastal regions in regard to circulation, mixing and biological activities emerge and dictate the efficiency of OAE.

3.2 Cumulative changes in CO_2 fluxes through the ocean surface

The second metric to calculate the CO_2 uptake efficiency is based on the changes in the air-sea CO_2 flux rather than DIC inventory change caused by the addition of alkalinity. The distribution of the water masses included in the efficiency calculation is smaller in the North Sea and at the coast of Norway for OAE applications in the North Sea (NE & BE, GER & DK) compared to the water masses tracked with a threshold of 50 μmol/kg (Fig. S3). For regions that are directly exposed to the Atlantic (ICE, NOR & SW, UK, except for IRE), the domains considered are larger than those used when tracking the alkalised water masses. The area detected in SP & PT expands even further westward into the Atlantic ocean. By calculating the cumulative fluxes of carbon and alkalinity over time, and from this the efficiency, the temporal variability in the efficiency is reduced, compared to efficiency calculations based on ΔDIC and ΔALK (vgl. Fig. S4). The diagnosed uptake efficiency reaches values between 0.31 (ICE) and 0.61 (FR) in 2047 (Table 1, Fig. 6c). Over the last 10 years of the OAE application, the efficiencies diagnosed from cumulative air-sea fluxes stay nearly constant, indicating that the system has reached a quasi-steady response, with carbon uptake continuing at an approximately constant efficiency.

3.3 Combined plume tracking

The area where the change in surface alkalinity exceeds a threshold and the air-sea flux change is statistically significant is much smaller than when the criteria are applied individually (Fig. S5). When the metric based on air-sea flux is applied to the area constraint by a threshold criterion of ΔALK>10 μmol/kg, the calculated uptake efficiency is higher for most simulations than calculated for only the threshold criterion (Tab. 2). In contrast, when the highest threshold is applied (ΔALK>100 μmol/kg) in

https://doi.org/10.5194/egusphere-2026-4781
Preprint. Discussion started: 18 August 2026

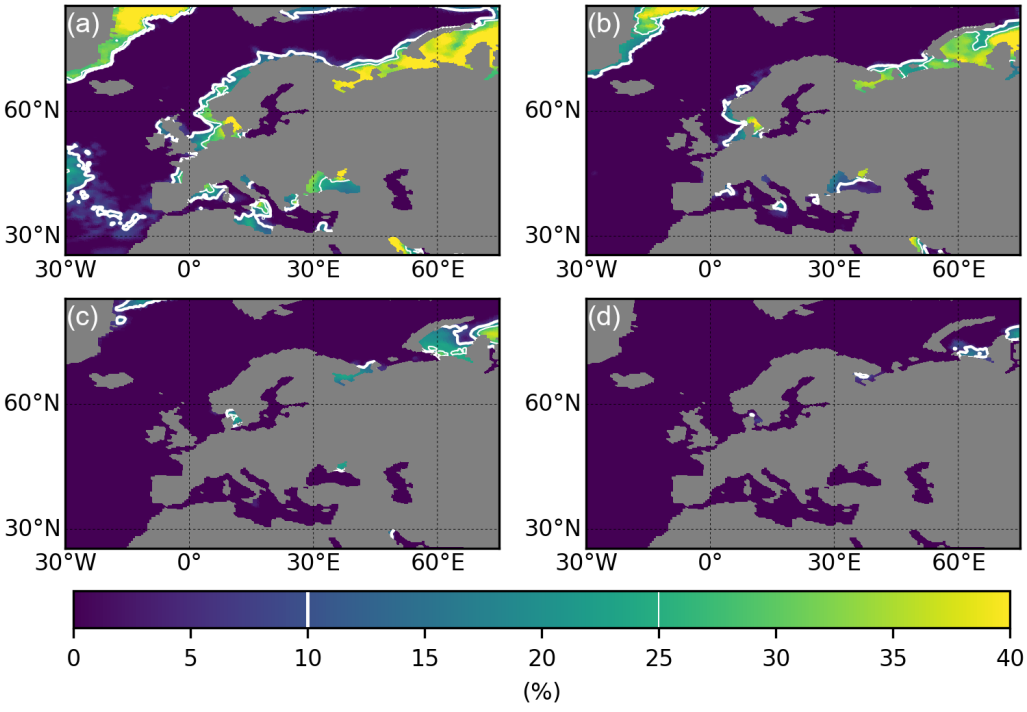

Figure 5. Probability density function (PDF) in BASE for surface alkalinity concentration to exceed the thresholds of (a) 10 μmol/kg, (b) 20 μmol/kg, (c) 50 μmol/kg, (d) 100 μmol/kg, with contour lines in white for 10% and 25% probability.

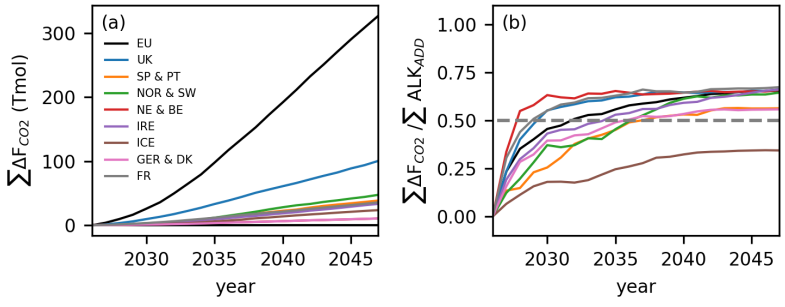

Figure 6. (a) Cumulative change in air-sea CO_2 flux in areas of significant increase in air-sea CO_2 flux connected to the deployment region. (b) Uptake efficiency. Horizontal dashed line at 0.5 for orientation.

addition to the air-sea flux criterion the uptake efficiency is always smaller than the calculated value for an area constraint by only the threshold criterion.

When the CO_2 uptake efficiency is calculated based on ΔDIC and ΔALK, temporal variability is in most cases of similar size or smaller than when only the threshold criterion is applied to constrain the area. The simulation for OAE application

https://doi.org/10.5194/egusphere-2026-4781
Preprint. Discussion started: 18 August 2026

Table 2. Mean CO_2 uptake efficiencies and temporal standard deviation calculated over the expanding plume of alkalised water based on four different thresholds to constrain the area applied to the surface alkalinity concentration.

	$\sum \Delta F_{CO_2} / \sum ALK_{ADD}$				$\Delta DIC / \Delta ALK$			
	10 μmol/kg	20 μmol/kg	50 μmol/kg	100 μmol/kg	10 μmol/kg	20 μmol/kg	50 μmol/kg	100 μmol/kg
EU	0.667	0.645	0.565	0.464	0.676±0.086	0.682±0.087	0.665±0.085	0.638±0.078
UK	0.666	0.653	0.610	0.536	0.651±0.066	0.648±0.068	0.630±0.058	0.599±0.048
SP&PT	0.570	0.524	0.330	0.129	0.568±0.131	0.540±0.125	0.484±0.113	0.432±0.065
NOR&SW	0.593	0.520	0.306	0.097	0.451±0.135	0.418±0.147	0.354±0.128	0.218±0.081
NE&BE	0.641	0.609	0.503	0.369	0.851±0.073	0.565±0.059	0.512±0.067	0.409±0.080
IRE	0.642	0.619	0.546	0.401	0.597±0.068	0.595±0.065	0.584±0.059	0.541±0.035
ICE	0.239	0.427	0.315	0.025	0.450±0.162	0.298±0.125	0.215±0.046	0.202±0.036
GER&DK	0.464	0.427	0.315	0.209	0.521±0.142	0.471±0.141	0.385±0.133	0.294±0.140
FR	0.707	0.688	0.650	0.557	0.601±0.109	0.622±0.116	0.609±0.101	0.571±0.100

around Iceland is the only exception. The temporal standard deviation, a representation of the temporal variability, increases for a threshold of 10 μmol/kg from 0.117 to 0.167. This increase in temporal variability is in one respect surprising, as the combination of criteria excludes the coast of Greenland, where the probability is high (>25 %) for the interannual variability to lead to an increase of the surface alkalinity by 20 μmol/kg or more (Fig. 5b).

4 Discussion

OAE works by deliberately increasing the alkalinity of the surface ocean to enhance CO_2 drawdown from the atmosphere. However, for the different metrics to measure the success of OAE in terms of oceanic carbon uptake or atmospheric CO_2 removal introduced in this study, the respective CO_2 uptake efficiencies are not consistent. In the following, we will discuss the reasons for the different results and provide recommendations in which context the different metrics might still be applied.

In contrast to other modelling studies addressing CO_2 uptake efficiency (Burt et al., 2021; He and Tyka, 2023; Tyka, 2025, e.g.), our model simulations are performed with a fully coupled ocean-land-atmosphere Earth system. In simulations without carbon coupling, i.e. with prescribed atmospheric CO_2 concentrations, all changes in alkalinity and DIC in the ocean are a direct result of OAE. With identical atmospheric CO_2 and hence identical climate, internal variability the baseline simulation and the OAE experiment would be identical apart from biogeochemical differences in the ocean (Schwinger et al., 2024). In a dynamically coupled climate model where atmospheric CO_2 responds to air-sea fluxes of CO_2 at the ocean surface, the addition of alkalinity enhances the draw-down of CO_2 from the atmosphere to the ocean. Some of that CO_2 can be emitted in other places when the water mass re-equilibrates with the atmosphere due to, e.g., changes in water temperature (Müller et al., 2025). Additionally, the reduction of global atmospheric CO_2 concentration can lead to changes in the air-sea and air-land fluxes all

https://doi.org/10.5194/egusphere-2026-4781
Preprint. Discussion started: 18 August 2026

over the globe (vlg. global change in land-air flux and sea-air flux of OAE simulations relative to BASE in Fig. S6; Keller et al., 2014, 2018; Schwinger et al., 2024).

While the feedbacks in coupled ocean-atmosphere systems and associated back-fluxes have been discussed and explained (Keller et al., 2014, 2018; Schwinger et al., 2024), our study reveals that these feedbacks can lead to phase shifts in the internal variability of the climate system. As has been shown in section 3.1, the phase shifts can be so substantial that the resulting effect on the global ocean DIC inventory may exceed the OAE-induced signal related to even relatively large amplitude regional OAE. This introduces additional uncertainty when referencing OAE impacts against a reference simulation (BASE) on annual to decadal timescales. For realistic, if on the higher end, amounts of alkalinity additions to the ocean, as applied in this study, on a timescale of 25 years feedback effects within the climate system are larger than the OAE signal in the carbon sequestration through DIC. Therefore, the global ocean budget changes in alkalinity and DIC are not a practical choice for efficiency calculations for regional OAE applications in an Earth system model that includes carbon-climate feedbacks and, by inference, in reality. However, it remains a useful quantity when applied to simulations without carbon coupling or when it can be shown that the effects of OAE are much greater than the internal variability.

When only the deployment region is considered for the calculation of changes in ocean alkalinity and DIC, the mean carbon uptake is underestimated (Fig. 7, yellow bar). This is caused by a combination of a long equilibration time, a short residence time of the alkalised water mass in the deployment region, and a small surface area at the coast. Because of the export of freshly DIC-enriched water out of the region, only a small portion of the total OAE-induced carbon uptake is accounted for by this regional approach (Fig. 4a). Accordingly, the calculated uptake efficiency with values between 0.16 and 0.53 underestimated the actual efficiency. The highest efficiency is calculated for the EU simulation, because the inclusion of the total European coast, on account of being deployment area, accounts for at least some of the lateral transport of the alkalised water along the Coast. In the other OAE simulations, the water mass would at that point leave the deployment region, and the DIC and Alkalinity contained therein is lost for the efficiency calculation. While the restriction of the calculation of ΔALK and ΔDIC to the deployment region underestimates the CO_2 uptake efficiency in our study, this criterion might still be applied, when OAE is deployed over a larger area and when export pathways are considered.

To account for the export of alkalised water, we apply a threshold approach to the surface alkalinity concentration changes between the OAE simulations and the reference simulation BASE to track the added alkalinity. The choice of threshold strongly affects the area included in the efficiency calculation and the ascertained carbon uptake efficiencies (Fig. 7, blue bars). He and Tyka (2023) showed the impact of general circulation patterns like coastal currents or downwelling, as well as atmospheric dynamics on the distribution and efficiency of OAE, which also need to be considered for threshold selection. Our results showed that for low thresholds, large parts of the Atlantic Ocean are included in the calculation, even if it is physically impossible for the alkalised water mass to reach that far within the simulated time frame. The high temporal variability in some regions in the North Sea and along the Norwegian coast also have an effect on the threshold selection, calling for higher thresholds than in regions with low temporal variability like the coasts of France or Ireland. The selection of an appropriate threshold results in an area that more closely resembles the expected plume shaped distribution of the alkalised water mass. While this method still can not track the total amount of the added alkalinity, it comes closer than constraining the model to

https://doi.org/10.5194/egusphere-2026-4781
Preprint. Discussion started: 18 August 2026

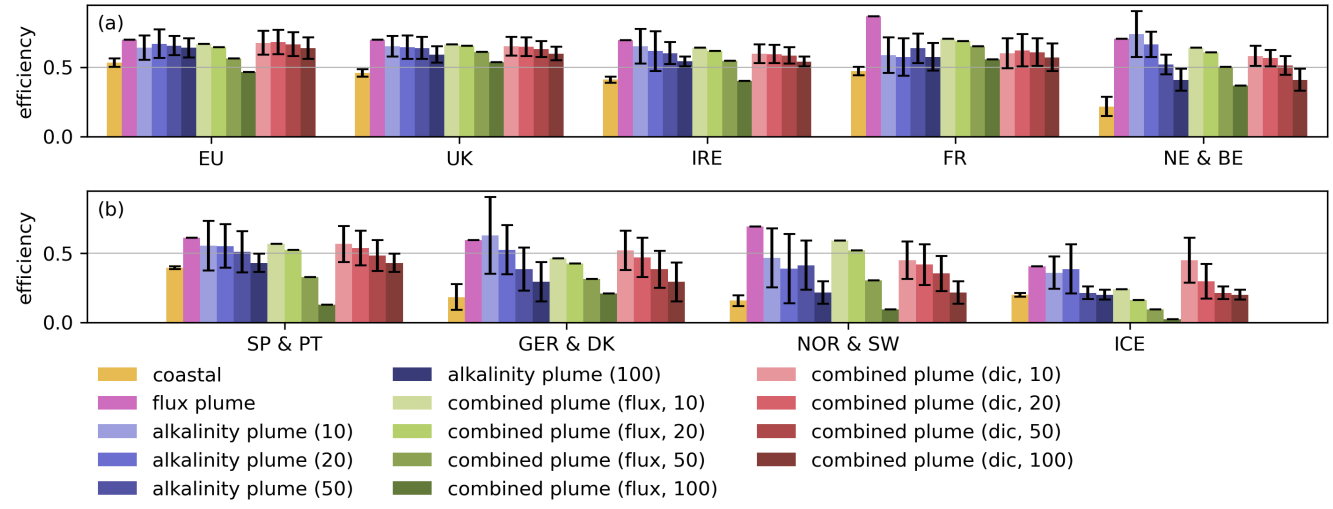

Figure 7. Mean CO_2 uptake efficiencies for different metrics and areas.

the deployment region. Water that leaves the surface area identified by the threshold criterion by moving below the surface is not tracked, which potentially underestimates the OAE induced changes in DIC.

Although the added alkalinity is generally more concentrated in the coastal deployment zones, the associated CO_2 uptake efficiency is lower there than when the plume is followed further offshore. The elevated alkalinity in the deployment area reduces seawater pCO_2, but the water's residence time in these coastal regions is too short to reach full equilibrium. As a result, a substantial portion of the CO_2 uptake occurs outside the original deployment areas (He and Tyka, 2023; Suselj et al., 2025), and the efficiencies computed for the threshold-defined alkalinity plumes are higher than those obtained when only the coastal deployment regions with elevated alkalinity are considered.

The calculation of efficiency via cumulative regional air-sea CO_2 flux differences has the advantage of capturing the cumulative CDR effect and naturally smooths temporal variability. Similar to ocean DIC, changes in the carbon flux through the ocean surface are affected by biological and chemical processes in the ocean. The effects of biological activity and its distribution in the ocean on pCO_2 introduce a factor of uncertainty. The use of ALK_{ADD} instead of ΔALK in the selected regions also has the advantage of removing the direct impact of the internal variability of the alkalinity in the equation, however, uncertainties in the air-sea CO_2 flux remain. Some areas like the subtropical Atlantic off the coast of Africa show high temporal variability and are close enough to the deployment region to be included in the plume tracking (EU, SP & PT in Fig. S4). In this particular case, the distribution of alkalised coastal water intersects with the Eastern North Atlantic Upwelling System, which extends along northwestern coast of Africa to the Atlantic coast of the Iberian Peninsula (Gómez-Gesteira et al., 2008). The upwelling of cold, nutrient-rich water fuels intense biological activity near the coast with strong interannual variability in meso-scale instabilities modulating the spatial distribution (Chavez and Messié, 2009; Lovecchio et al., 2017, 2018). Therefore, the ap-

https://doi.org/10.5194/egusphere-2026-4781
Preprint. Discussion started: 18 August 2026

plication of OAE in or near upwelling systems needs to be carefully considered with regard to monitoring and attribution of carbon uptake.

To further reduce uncertainties from variability of the surface alkalinity and biological activity, a combination of the two plume tracking mechanisms has been applied. The resulting area only includes regions where an increase in surface alkalinity leads to a significant increase in carbon uptake by the ocean. This method allows the exclusion of areas with high alkalinity increase but no additional carbon uptake, as well as regions with stronger carbon uptake but no change in surface alkalinity and therefore not caused by OAE. When the CO_2 uptake efficiency is calculated based on the cumulative carbon flux in the resulting regions, the mean efficiency shows a stronger dependency on the alkalinity threshold than if only the threshold criterion is applied (Fig. 7, green bars). When the efficiency is calculated based on ΔDIC and ΔALK (Fig. 7, red bars), the threshold dependency is smaller in most OAE simulations because, while alkalised water masses can still be excluded from the detected area, parts of the accumulated carbon in this water mass is excluded as well, partially balancing the alkalinity loss. The combined plume areas criterion is the most robust method of the ones applied in this study to track the alkalised water mass, as it reduces the two largest sources of uncertainty. However, the threshold selection for the change in surface alkalinity concentration still needs to be considered in regard to natural variability and independently for each deployment region.

The atmospheric concentration of CO_2 is the part of the climate system that any method of carbon dioxide removal needs to target. A method that has been proposed to calculate the uptake efficiency is based on the change in CO_2 concentration relative to the added alkalinity (Jeltsch-Thömmes et al., 2025; Grosselindemann et al., 2026). This would allow a direct assessment of the impact of OAE or other CDR methods on the climate. However, the total amount of atmospheric carbon removal caused by regional coastal-European OAE is, on annual to multi-decadal timescales not discernible from changes in the atmospheric CO_2 concentration caused by changing climate patterns. This result is similar to the approach of measuring the global oceanic DIC increase, while atmospheric CO_2 is additionally affected by fluctuating terrestrial carbon fluxes, such as the temporary weakening of the land carbon sink during El Niño, which is much larger on the simulated time scales than the effect of OAE, obscuring the additional uptake of carbon by the ocean (Bastos et al., 2018). On such timescales, changes in atmospheric CO_2 concentration are therefore not a sensitive measure for OAE efficiency, neither in fully coupled Earth system models as used here, nor in the real world. Similarly to the efficiency metric based on global-ocean ΔDIC, this metric can be applied to simulations without carbon feedback that avoid changes in the climate system, or that have very large alkalinity additions for many decades (Keller et al., 2018; Jeltsch-Thömmes et al., 2025).

Lastly, the application of OAE in an SSP3-7.0 emission scenario is not ideal because OAE only makes sense in a climate-policy view, when the large majority of current emissions have been reduced and OAE and other CDR methods have a chance to compensate for the hard-to-abate residual emissions. The effects of phase shifts in internal climate modes on air-sea CO_2 fluxes and associated changes in atmospheric and oceanic carbon inventories can for many years to decades be larger than the CO_2 fluxes into the ocean brought about by even relatively large regional OAE deployment (e.g. EU). Therefore, it is not surprising that the effects of regional OAE on global CO_2 concentrations are rather small and any impact on the climate system in the current SSP3-7.0 emission scenario will only become visible after many decades.

https://doi.org/10.5194/egusphere-2026-4781
Preprint. Discussion started: 18 August 2026

5 Conclusions

In this study, we compared multiple approaches to calculate the CO_2 uptake efficiency for regional ocean alkalinity enhancement (OAE) using an Earth system model with additions of alkalinity of potentially realistic and feasible amounts along European coasts.

Previous studies have applied the metrics presented in this study in a model setting without a fully interactive carbon system, so related feedbacks where not relevant for the interpretation of the metrics (Burt et al., 2021; He and Tyka, 2023; Nagwekar et al., 2024). Alternatively, very large quantities of alkalinity are added to the ocean that have a larger impact on the carbon system than any feedback effects (Jeltsch-Thömmes et al., 2025). We showed that for smaller amounts of OAE that are closer to practical implementation, several commonly used methods for determining CO_2 uptake efficiency are not suitable. Calculating the efficiency based on global inventory changes of alkalinity and DIC is affected strongly by shifts in the climate system, while internal variability of the surface ocean lead to biases when tracking the distribution of the added alkalinity or the OAE-induced strengthening of the air-sea CO_2 flux. The choice of metric therefore needs to be considered carefully for each experiment based on (i) the local ocean conditions in the deployment region, (ii) the temporal variability of the surface alkalinity and air-sea CO_2 flux, and (iii) to possible impacts on global climate modes such as El Niño.

However, a full quantitative comparison of these metrics is not possible within the present model setup. Such an assessment would require dedicated tracers for added alkalinity and the associated DIC changes in order to better isolate the OAE signal from background variability and secondary climate effects. These tracers are planned for in future simulations and will provide a stronger basis for evaluating the performance of the different metrics. In addition, ensemble simulations will be needed to better constrain the signal-to-noise ratio and to assess the robustness of the diagnosed efficiency. Together, these developments will help to determine which metric provides the most reliable criterion for realistic OAE applications under which conditions or for which regions.

Generally, OAE experiments in Earth system modelling encounter similar uncertainties as real-world applications such as interannual variability and feedback effects. However, there is no "second Earth" as a counterfactual in field experiments. Although modelling makes it possible to introduce tracers to follow the impacts of OAE, this study deliberately avoided using extra tracers for the added alkalinity and OAE-driven carbon uptake, in order to better illustrate both the potential and the challenges of employing Earth system models for monitoring, reporting and verification (MRV).

Although alkalinity and DIC are principally straightforward to measure, it is technically not possible to have global data coverage for both parameters on temporal and/or spatial resolutions that allow for comparison to global inventory changes in models (and as we have shown, the usage of global inventory changes is limited in its usefulness). Plume tracking is more feasible in terms of comparability to measurements because the alkalised water plume covers a much smaller area, however, the potential to over- or underestimate the efficiency is high. In contrast to global budgeting of DIC and alkalinity changes, this method would allow a spatially resolved comparison between modelling results and monitoring of experimental setups. The measurement of air-sea CO_2 fluxes through the ocean surface is technically possible, but for long term application, constant monitoring would be required. And while this method seems to be the most robust for regional OAE in Earth system modelling,

https://doi.org/10.5194/egusphere-2026-4781
Preprint. Discussion started: 18 August 2026

it is not necessarily the best metric in real-world applications. In contrast to ocean DIC, the integrated carbon flux into the ocean only represents the additional uptake of carbon at a given time while the change in DIC represents the net change, including carbon gain and loss through the surface and biological processes in the ocean's interior.

The spreading area of the alkalised water does not consider boundaries between countries, but the addition of alkalinity in the coastal waters of one country might affect the potential for OAE of its neighbours (He and Tyka, 2023). It is therefore important to know and track the distribution patterns of the affected water masses to avoid potential conflicts.

Code and data availability. The code for FOCI-MOPS can be accessed from the ESM tools at https://zenodo.org/doi/10.5281/zenodo.3737927 (Gierz et al., 2021). The Python codes used for the analysis of the model output will be make available upon request to the corresponding author. A processed minimum data set of the FOCI-MOPS data will be available at the time of publication. The full model simulation dataset, which spans several terabytes, will be provided by the corresponding author upon request.

Author contributions. TK ran the model simulations. VT and TK performed the analysis. All authors contributed to the interpretation of the results. VT wrote the initial draft. All authors contributed to reviewing and editing of the text.

Competing interests. The authors declare that they have no conflict of interest

Acknowledgements. This work was done as part of project Ocean Alk-Align, funded by Carbon to Sea and the Thistledown Foundation. Computing time was provided by the former computing center HLRN Berlin, now NHR@ZIB. The computing time was funded by European Union's Horizon 2020 research and innovation program under grant agreement no. 869357 (OceanNets). The research was also supported by the German Federal Ministry of Research, Technology and Space (BMFTR) in the framework of RETAKE-II (project number 03F0965), one of the five research consortia of the German Marine Research Alliance (DAM) research mission »Marine carbon sinks in decarbonisation pathways (CDRmare)«. The analysis was performed on HPC NESH at University of Kiel.

https://doi.org/10.5194/egusphere-2026-4781
Preprint. Discussion started: 18 August 2026

References

Bastos, A., Friedlingstein, P., Sitch, S., Chen, C., Mialon, A., Wigneron, J.-P., Arora, V. K., Briggs, P. R., Canadell, J. G., Ciais, P., Chevallier, F., Cheng, L., Delire, C., Haverd, V., Jain, A. K., Joos, F., Kato, E., Lienert, S., Lombardozzi, D., Melton, J. R., Myneni, R., Nabel, J. E. M. S., Pongratz, J., Poulter, B., Rödenbeck, C., Séférian, R., Tian, H., van Eck, C., Viovy, N., Vuichard, N., Walker, A. P., Wiltshire, A., Yang, J., Zaehle, S., Zeng, N., and Zhu, D.: Impact of the 2015/2016 El Niño on the terrestrial carbon cycle constrained by bottom-up and top-down approaches, Philosophical Transactions of the Royal Society B: Biological Sciences, 373, 20170 304, https://doi.org/10.1098/rstb.2017.0304, 2018.

Burgess, M., Becker, S., Langendorf, R., Fredston, A., and Brooks, C.: Climate change scenarios in fisheries and aquatic conservation research, ICES J. Mar. Sci., 80, 1163–1178, 2023.

Burt, D. J., Fröb, F., and Ilyina, T.: The Sensitivity of the Marine Carbonate System to Regional Ocean Alkalinity Enhancement, Frontiers in Climate, 3, 3:624 075, https://doi.org/10.3389/fclim.2021.624075, 2021.

Canadell, J., Monteiro, P., Costa, M., da Cunha, L. C., Cox, P., Eliseev, A., S. Henson, M. I., Jaccard, S., Koven, C., Lohila, A., Patra, P., Piao, S., Rogelj, J., Syampungani, S., Zaehle, S., and Zickfeld, K.: Global Carbon and other Biogeochemical Cycles and Feedbacks, in: In Climate Change 2021: The Physical Science Basis. Contribution of Working Group I to the Sixth Assessment Report of the Intergovernmental Panel on Climate Change, edited by Masson-Delmotte, V., Zhai, P., Pirani, A., Connors, S., Péan, C., Berger, S., Caud, N., Chen, Y., Goldfarb, L., Gomis, M., Huang, M., Leitzell, K., Lonnoy, E., Matthews, J., Maycock, T., Waterfield, T., Yelekçi, O., Yu, R., and Zhou, B., p. 673–816, Cambridge University Press, Cambridge, United Kingdom and New York, NY, USA, https://doi.org/10.1017/9781009157896.007, 2021.

CEMBUREAU: The Economy, in: Activity Report 2022, https://www.cementeurope.eu/media/3oabmi0i/cembureau-activity-report-2022-web.pdf, 2023.

Chavez, F. P. and Messié, M.: A comparison of Eastern Boundary Upwelling Ecosystems, Prog. Oceanogr., pp. 80–96, https://doi.org/10.1016/j.pocean.2009.07.032, 2009.

Chien, C.-T., Durgadoo, J. V., Ehlert, D., Frenger, I., Keller, D. P., Koeve, W., Kriest, I., Landolfi, A., Patara, L., Wahl, S., and Oschlies, A.: FOCI-MOPS v1 - integration of marine biogeochemistry within the Flexible Ocean and Climate Infrastructure version 2 (FOCI 1) Earth systemmodel, Geosci. Model Dev., pp. 5987–6024, https://doi.org/10.5194/gmd-15-5987-2022, 2022.

Foteinis, S., Andresen, J., Campo, F., Caserini, S., and Renforth, P.: Life cycle assessment of ocean liming for carbon dioxide removal from the atmosphere, Journal of Cleaner Production, 370, 133 309, https://doi.org/10.1016/j.jclepro.2022.133309, 2022.

Friedlingstein, P., Jones, M. W., O'Sullivan, M., Andrew, R. M., Bakker, D. C. E., Hauck, J., Quéré, C. L., Peters, G. P., Peters, W., Pongratz, J., Sitch, S., Canadell, J. G., Ciais, P., Jackson, R. B., Alin, S. R., Anthoni, P., Bates, N. R., Becker, M., Bellouin, N., Bopp, L., Chau, T. T. T., Chevallier, F., Chini, L. P., Cronin, M., Currie, K. I., Decharme, B., Djeutchouang, L. M., Dou, X., Evans, W., Feely, R. A., Feng, L., Gasser, T., Gilfillan, D., Gkritzalis, T., Grassi, G., Gregor, L., Gruber, N., Özgür Gürses, Harris, I., Houghton, R. A., Hurtt, G. C., Iida, Y., Ilyina, T., Luijkx, I. T., Jain, A., Jones, S. D., Kato, E., Kennedy, D., Goldewijk, K. K., Knauer, J., Korsbakken, J. I., Körtzinger, A., Landschützer, P., Lauvset, S. K., Lefèvre, N., Lienert, S., Liu, J., Marland, G., McGuire, P. C., Melton, J. R., Munro, D. R., Nabel, J. E. M. S., Nakaoka, S.-I., Niwa, Y., Ono, T., Pierrot, D., Poulter, B., Rehder, G., Resplandy, L., Robertson, E., Rödenbeck, C., Rosan, T. M., Schwinger, J., Schwingshackl, C., Séférian, R., Sutton, A. J., Sweeney, C., Tanhua, T., Tans, P. P., Tian, H., Tilbrook, B., Tubiello, F., van der Werf, G. R., Vuichard, N., Wada, C., Wanninkhof, R., Watson, A. J., Willis, D., Wiltshire, A. J., Yuan, W., Yue, C., Yue, X.,

https://doi.org/10.5194/egusphere-2026-4781
Preprint. Discussion started: 18 August 2026

Zaehle, S., and Zeng, J.: Global Carbon Budget 2021, Earth System Science Data, 14, 1917–2005, https://doi.org/10.5194/essd-14-1917-2022, 2022.

Gierz, P., Andrés-Martínez, M., Barbi, D., Wieters, N., Cristini, L., Streffing, J., Wahl, S., Ural, D., Kjellsson, J., Chegini, F., , and Khosravi, S.: ESM-Tools, https://doi.org/10.5281/zenodo.5787476, zenodo, [software], 2021.

Grosselindemann, H., Burger, F. A., and Frölicher, T. L.: The efficiency and ocean acidification mitigation potential of ocean alkalinity enhancement on multi-centennial timescales, Biogeosciences, 23, 3299–3321, https://doi.org/10.5194/bg-23-3299-2026, 2026.

Gómez-Gesteira, M., De Castro, M., Álvarez, I., Lorenzo, M. N., Gesteira, J. L. G., and Crespo, A. J. C.: Spatio-temporal Upwelling Trends along the Canary Upwelling System (1967–2006), Annals of the New York Academy of Sciences, 1146, 320–337, https://doi.org/10.1196/annals.1446.004, 2008.

He, J. and Tyka, M. D.: Limits and CO_2 equilibration of near-coast alkalinity enhancement, Biogeosciences, 20, 27–43, https://doi.org/10.5194/bg-20-27-2023, 2023.

Jeltsch-Thömmes, A., Tran, G., Lienert, S., Keller, D., Oschlies, A., and Joos, F.: Earth system responses to carbon dioxide removal as exemplified by ocean alkalinity enhancementL tradeoffs and lags, Environmental Research Letters, 19, 054 054, https://doi.org/10.1088/1748-9326/ad4401, 2025.

Keller, D. P., Feng, E. Y., and Oschlies, A.: Potential climate engineering effectiveness and side effects during a high carbon dioxide-emission scenario, Nature Communications, 5, 3304, https://doi.org/10.1038/ncomms4304, 2014.

Keller, D. P., Lenton, A., Littleton, E. W., Oschlies, A., Scott, V., and Vaughan, N. E.: The Effects of Carbon Dioxide Removal on the Carbon Cycle, https://doi.org/10.1007/s40641-018-0104-3, 2018.

Kriest, I. and Oschlies, A.: MOPS-1.0: towards a model for the regulation of the global oceanic nitrogen budget by marine biogeochemical processes, Geosci. Model Dev., pp. 2929–2957, https://doi.org/10.5194/gmd-8-2929-2015, 2015.

Liddicoat, S. K., Wiltshire, A. J., Jones, C. D., Arora, V. K., Brovkin, V., Cadule, P., Hajima, T., Lawrence, D. M., Pongratz, J., Schwinger, J., Séférian, R., Tjiputra, J. F., and Ziehn, T.: Compatible Fossil Fuel CO2 Emissions in the CMIP6 Earth System Models' Historical and Shared Socioeconomic Pathway Experiments of the Twenty-First Century, Journal of Climate, 34, 2853–2875, https://doi.org/10.1175/JCLI-D-19-0991.1, 2021.

Lovecchio, E., Gruber, N., Münnich, M., and Lachkar, Z.: On the long-range offshore transport of organic carbon from the Canary Upwelling System to the open North Atlantic, Biogeosciences, 14, 3337–3369, https://doi.org/10.5194/bg-14-3337-2017, 2017.

Lovecchio, E., Gruber, N., , and Münnich, M.: Mesoscale contribution to the long-range offshore transport of organic carbon from the Canary Upwelling System to the open North Atlantic, Biogeosciences, 15, 5061–5091, https://doi.org/10.5194/bg-15-5061-2018, 2018.

Madec, G. and the NEMO team: NEMO ocean engine, Note du Pôle modélisation, Inst. Pierre-Simon Laplace No 27, 2016.

Matthes, K., Biastoch, A., Wahl, S., Harlaß, J., Martin, T., Brücher, T., Drews, A., Ehlert, D., Getzlaff, K., Krüger, F., Rath, W., Scheinert, M., Schwarzkopf, F. U., Bayr, T., Schmidt, H., and Park, W.: The Flexible Ocean and Climate Infrastructure version 1 (FOCI1): mean state and variability, Geosci. Model Dev., pp. 2533–2568, https://doi.org/10.5194/gmd-13-2533-2020, 2020.

Meinshausen, M., Nicholls, Z. R., Lewis, J., Gidden, M. J., Vogel, E., and Freund, M. e. a.: The shared socio-economic pathway (SSP) greenhouse gas concentrations and their extensions to 2500, Geoscientific Model Development, 13(8), 3571–3605, https://doi.org/10.5194/gmd-13-3571-2020, 2020.

Müller, J. D., Bakker, D. C. E., Gruber, N., Schneuwly, A., Gehlen, M., Gregor, L., Hauck, J., Landschützer, P., and McKinley, G. A.: Unexpected decline in the ocean carbon sink under record-high sea surface temperatures in 2023, Nature Climate Change, 15, 978–985, https://doi.org/10.1038/s41558-025-02380-4, 2025.

https://doi.org/10.5194/egusphere-2026-4781
Preprint. Discussion started: 18 August 2026

Nagwekar, T., Nissen, C., and Hauck, J.: Ocean Alkalinity Enhancement in Deep Water Formation Regions Under Low and High Emission Pathways, Earth's Future, 12, e2023EF004 213, https://doi.org/10.1029/2023EF004213, 2024.

Oschlies, A., Bach, L. T., Fennel, K., Gattuso, J.-P., and Mengis, N.: Perspectives and challenges of marine carbon dioxide removal, Frontiers in Climate, 6, 1506 181, https://doi.org/10.3389/fclim.2024.1506181, 2025.

Paulmier, A., Kriest, I., and Oschlies, A.: Stoichiometries of remineralisation and denitrification in global biogeochemical ocean models, Biogeosciences, 6, 923–935, https://doi.org/10.5194/bg-6-923-2009, 2009.

Pelz, M.-T. and Slawig, T.: Diffusion-based kernel density estimator (diffKDE) (Version 0.0.2), https://doi.org/10.5281/zenodo.13736609, zenodo [Computer software], 2024.

Pelz, M.-T., Schartau, M., Somes, C. J., Lampe, V., and Slawig, T.: A diffusion-based kernel density estimator (diffKDE, version 1) with optimal bandwidth approximation for the analysis of data in geoscience and ecological research, Geoscientific Model Development, 16, 6609–6634, https://doi.org/10.5194/gmd-16-6609-2023, 2023.

Renforth, P. and Henderson, G.: Assessing ocean alkalinity for carbon sequestration, Reviews of Geophysics, 55, 636–674, https://doi.org/10.1002/2016RG000533, 2017.

Riahi, K., van Vuuren, D. P., Kriegler, E., Edmonds, J., O'Neill, B. C., Fujimori, S., Bauer, N., Calvin, K., Dellink, R., Fricko, O., Lutz, W., Popp, A., Cuaresma, J. C., KC, S., Leimbach, M., Jiang, L., Kram, T., Rao, S., Emmerling, J., Ebi, K., Hasegawa, T., Havlik, P., Humpenöder, F., Da Silva, L. A., Smith, S., Stehfest, E., Bosetti, V., Eom, J., Gernaat, D., Masui, T., Rogelj, J., Strefler, J., Drouet, L., Krey, V., Luderer, G., Harmsen, M., Takahashi, K., Baumstark, L., Doelman, J. C., Kainuma, M., Klimont, Z., Marangoni, G., Lotze-Campen, H., Obersteiner, M., Tabeau, A., and Tavoni, M.: The Shared Socioeconomic Pathways and their energy, land use, and greenhouse gas emissions implications: An overview, Global Environmental Change, 42, 153–168, https://doi.org/https://doi.org/10.1016/j.gloenvcha.2016.05.009, 2017.

Schwinger, J., Bourgeois, T., and Rickels, W.: On the emission-path dependency of the efficiency of ocean alkalinity enhancement, Environmental Research Letters, 19, https://doi.org/10.1088/1748-9326/ad5a27, 2024.

Stevens, B., Giorgetta, M., Esch, M., Mauritsen, T., Crueger, T., Rast, S., Salzmann, M., Schmidt, H., Bader, J., Block, K., Brokopf, R., Fast, I., Kinne, S., Kornblueh, L., Lohmann, U., Pincus, R., Reichler, T., and Roeckner, E.: Atmospheric component of the MPI-M earth system model: ECHAM6, Journal of Advances in Modeling Earth Systems, 5, 146–172, https://doi.org/10.1002/jame.20015, 2013.

Sun, C., Liao, E., and Zhu, X.: Asymmetrical Ocean Carbon Responses in the Tropical Pacific Ocean to La Niña and El Niño, Geophysical Research Letters, 52, e2024GL112 039, https://doi.org/10.1029/2024GL112039, 2025.

Suselj, K., Carroll, D., Whitt, D., Samuels, B., Menemenlis, D., Zhang, H., Beatty, N., and Savage, A.: Quantifying Marine Carbon Dioxide Removal via Alkalinity Enhancement Across Circulation Regimes Using ECCO-Darwin and 1D Models, Journal of Advances in Modeling Earth Systems, 17, https://doi.org/10.1029/2024MS004847, 2025.

Turk, D., Wang, H., Hu, X., Gledhill, D. K., Wang, Z. A., Jiang, L., and Cai, W.-J.: Time of Emergence of Surface Ocean Carbon Dioxide Trends in the North American Coastal Margins in Support of Ocean Acidification Observing System Design, Frontiers in Marine Science, 6, https://doi.org/10.3389/fmars.2019.00091, 2019.

Tyka, M. D.: Efficiency metrics for ocean alkalinity enhancements under responsive and prescribed atmospheric pCO_2 conditions, Biogeosciences, 22, 341–353, https://doi.org/10.5194/bg-22-341-2025, 2025.

UNFCCC: Adoption of the Paris Agreement, https://unfccc.int/resource/docs/2015/cop21/eng/l09r01.pdf, 2015.

United Nations Environment Programme: Emissions Gap Report 2025: Off target – Continued collective inaction puts global temperature goal at risk, Noirobi, https://doi.org/10.59117/20.500.11822/48854, 2025.